Supplemental Document

Optics EXPRESS

# Diffraction-optimized aperiodic surface structures for enhanced current density in organic solar cells: supplement

**M. MERKEL,* J. IMBROCK, AND C. DENZ**

*Institute of Applied Physics, University of Muenster, Corrensstr. 2/4, 48149 Muenster, Germany*
**mmerkel@uni-muenster.de*



Supplement DOI: https://doi.org/10.6084/m9.figshare.20330658

Parent Article DOI: https://doi.org/10.1364/OE.465177

# Diffraction-optimized aperiodic Surface Structures for enhanced Current Density in Organic Solar Cells: supplemental document

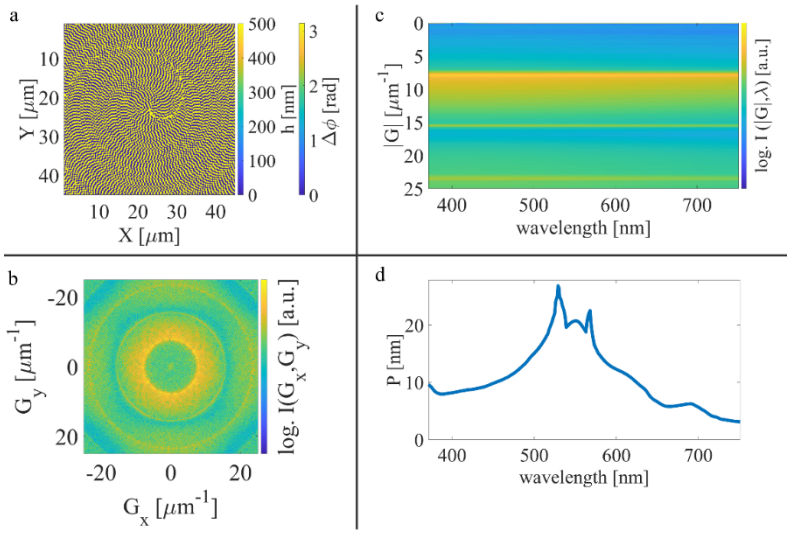


Fig. S1. Visualization of steps for calculating the path length elongation using the example of a periodic sequence on rings. a) Surface relief for a relief height h of 500 nm and a diameter of 500 nm, as well as phase difference between light incident on the pillars and on the grooves for $\lambda = 400$ nm. b) Intensity distribution of spatial frequencies $G_x$ and $G_y$ of the phase grating in x- and y-direction. c) Intensity distribution of absolute value of spatial frequency, |G|, for wavelengths between 370 nm and 750 nm. d) Active path elongation.

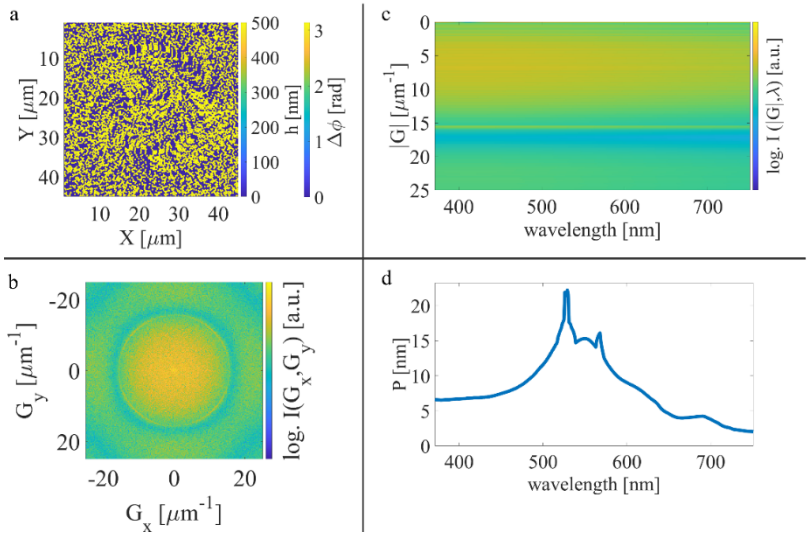


Fig. S2. Visualization of steps for calculating the path length elongation using the example of the Rudin-Shapiro sequence on rings. a) Surface relief for a relief height h of 500 nm and a diameter of 500 nm, as well as phase difference between light incident on the pillars and on the grooves for $\lambda = 400$ nm. b) Intensity distribution of spatial frequencies $G_x$ and $G_y$ of the phase grating in x- and y-direction. c) Intensity distribution of absolute value of spatial frequency, |G|, for wavelengths between 370 nm and 750 nm. d) Active path elongation.

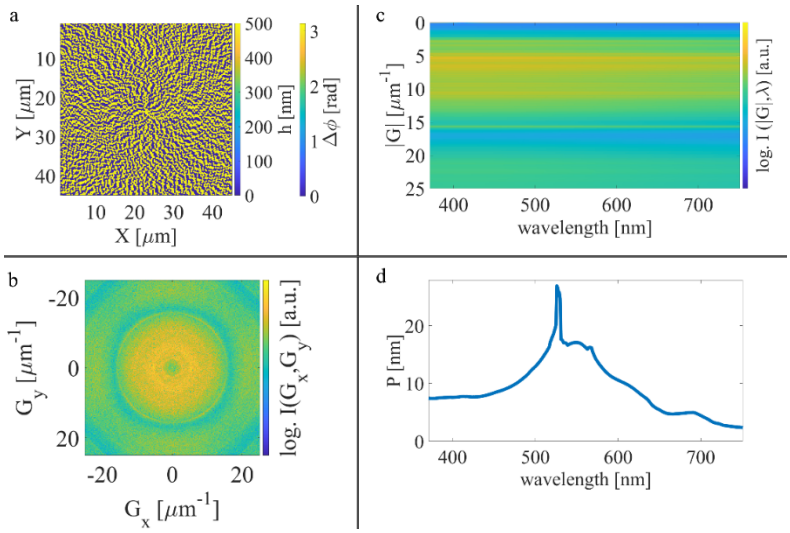


Fig. S3. Visualization of steps for calculating the path length elongation using the example of the Thue-Morse sequence on rings. a) Surface relief for a relief height h of 500 nm and a diameter of 500 nm, as well as phase difference between light incident on the pillars and on the grooves for $\lambda = 400$ nm. b) Intensity distribution of spatial frequencies $G_x$ and $G_y$ of the phase grating in x- and y-direction. c) Intensity distribution of absolute value of spatial frequency, |G|, for wavelengths between 370 nm and 750 nm. d) Active path elongation.

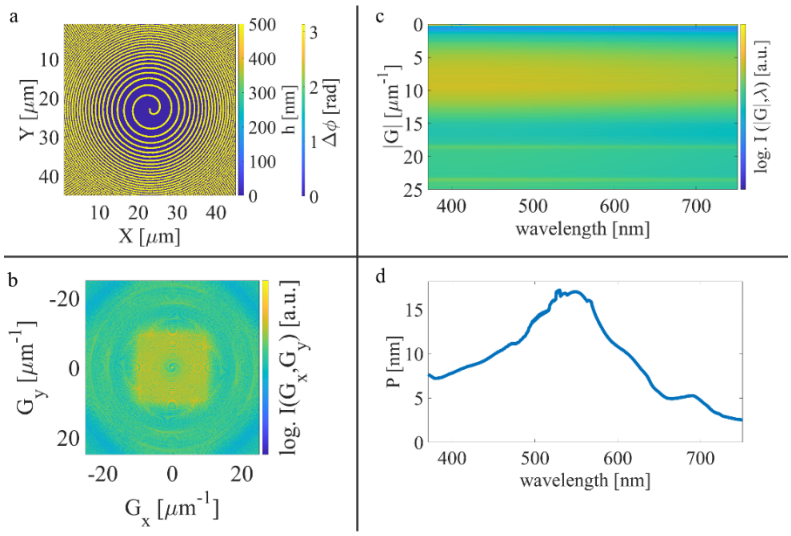


Fig. S4. Visualization of steps for calculating the path length elongation using the example of a periodic sequence on a Fermat's spiral. a) Surface relief for a relief height h of 500 nm and a diameter of 500 nm, as well as phase difference between light incident on the pillars and on the grooves for $\lambda = 400$ nm. b) Intensity distribution of spatial frequencies $G_x$ and $G_y$ of the phase grating in x- and y-direction. c) Intensity distribution of absolute value of spatial frequency, |G|, for wavelengths between 370 nm and 750 nm. d) Active path elongation.

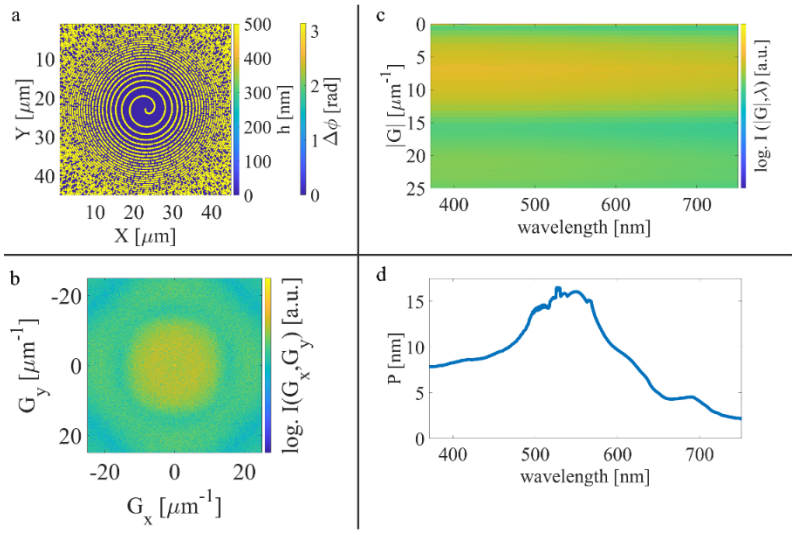


Fig. S5. Visualization of steps for calculating the path length elongation using the example of the Rudin-Shapiro sequence on a Fermat's spiral. a) Surface relief for a relief height h of 500 nm and a diameter of 500 nm, as well as phase difference between light incident on the pillars and on the grooves for $\lambda = 400$ nm. b) Intensity distribution of spatial frequencies $G_x$ and $G_y$ of the phase grating in x- and y-direction. c) Intensity distribution of absolute value of spatial frequency, |G|, for wavelengths between 370 nm and 750 nm. d) Active path elongation.

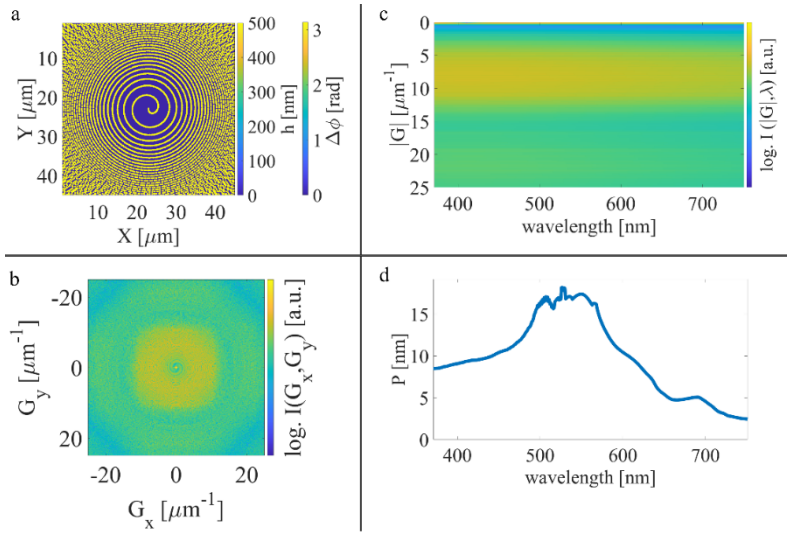


Fig. S6. Visualization of steps for calculating the path length elongation using the example of the Thue-Morse sequence on a Fermat's spiral. a) Surface relief for a relief height h of 500 nm and a diameter of 500 nm, as well as phase difference between light incident on the pillars and on the grooves for $\lambda = 400$ nm. b) Intensity distribution of spatial frequencies $G_x$ and $G_y$ of the phase grating in x- and y-direction. c) Intensity distribution of absolute value of spatial frequency, |G|, for wavelengths between 370 nm and 750 nm. d) Active path elongation.

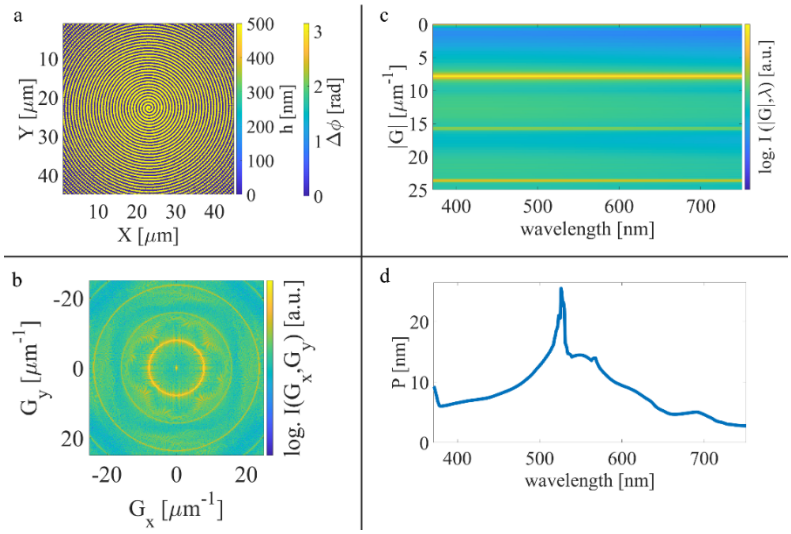


Fig. S7. Visualization of steps for calculating the path length elongation using the example of a periodic sequence on an Archimedean spiral. a) Surface relief for a relief height h of 500 nm and a diameter of 500 nm, as well as phase difference between light incident on the pillars and on the grooves for $\lambda = 400$ nm. b) Intensity distribution of spatial frequencies $G_x$ and $G_y$ of the phase grating in x- and y-direction. c) Intensity distribution of absolute value of spatial frequency, |G|, for wavelengths between 370 nm and 750 nm. d) Active path elongation.

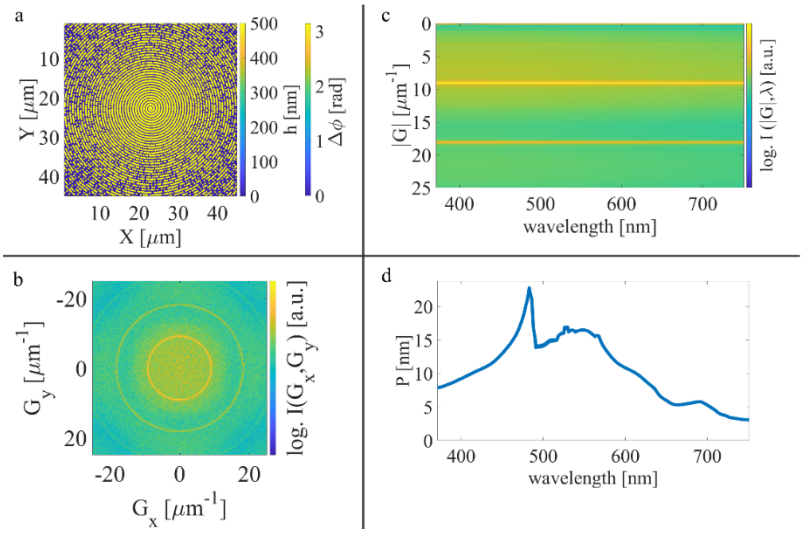


Fig. S8. Visualization of steps for calculating the path length elongation using the example of the Rudin-Shapiro sequence on an Archimedean spiral. a) Surface relief for a relief height h of 500 nm and a diameter of 500 nm, as well as phase difference between light incident on the pillars and on the grooves for $\lambda = 400$ nm. b) Intensity distribution of spatial frequencies $G_x$ and $G_y$ of the phase grating in x- and y-direction. c) Intensity distribution of absolute value of spatial frequency, |G|, for wavelengths between 370 nm and 750 nm. d) Active path elongation.

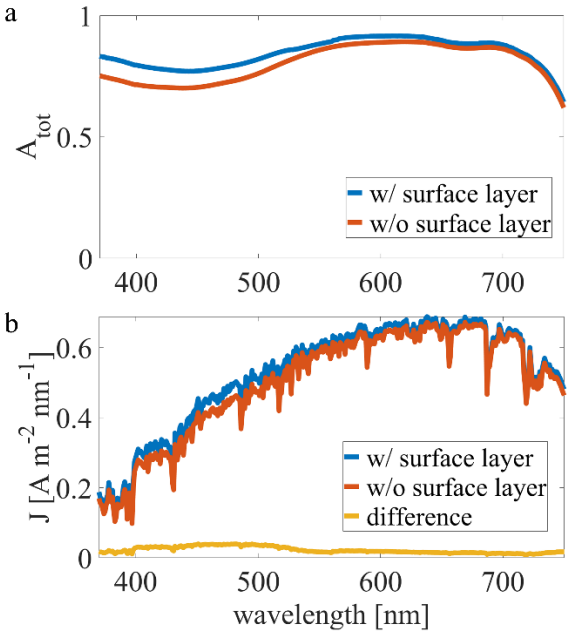


Fig. S9. Periodic sequence on rings. a) Total absorption in the active layer with and without surface layer. b) Spectral current density with and without surface layer and the difference between the two.

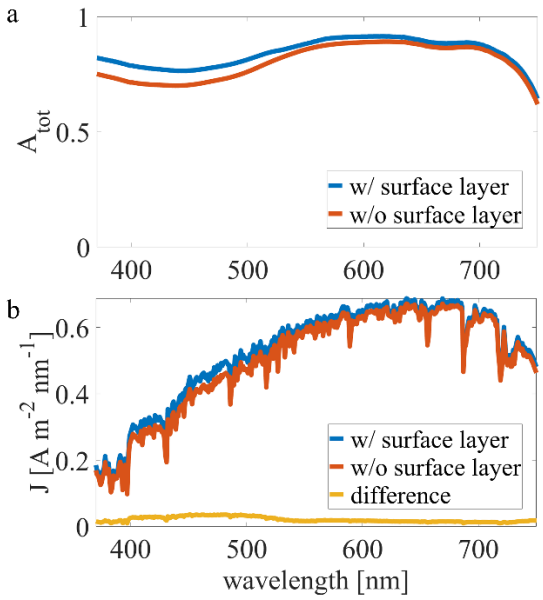


Fig. S10. Rudin-Shapiro sequence on rings. a) Total absorption in the active layer with and without surface layer. b) Spectral current density with and without surface layer and the difference between the two.

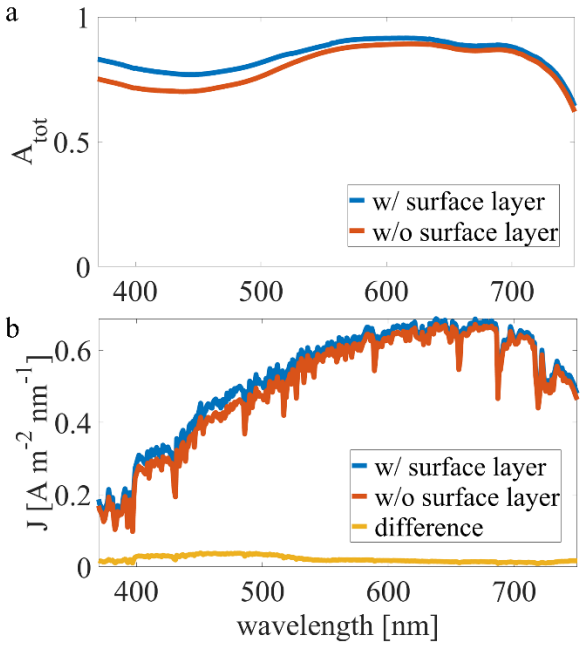


Fig. S11. Thue-Morse sequence on rings. a) Total absorption in the active layer with and without surface layer. b) Spectral current density with and without surface layer and the difference between the two.

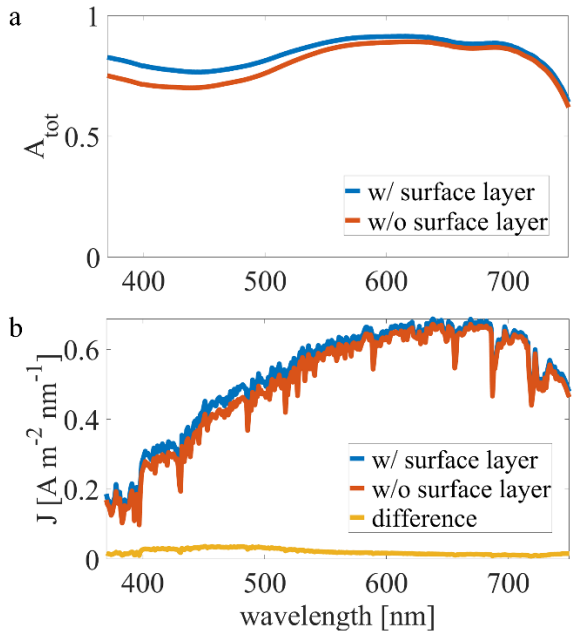


Fig. S12. Periodic sequence on a Fermat's spiral. a) Total absorption in the active layer with and without surface layer. b) Spectral current density with and without surface layer and the difference between the two.

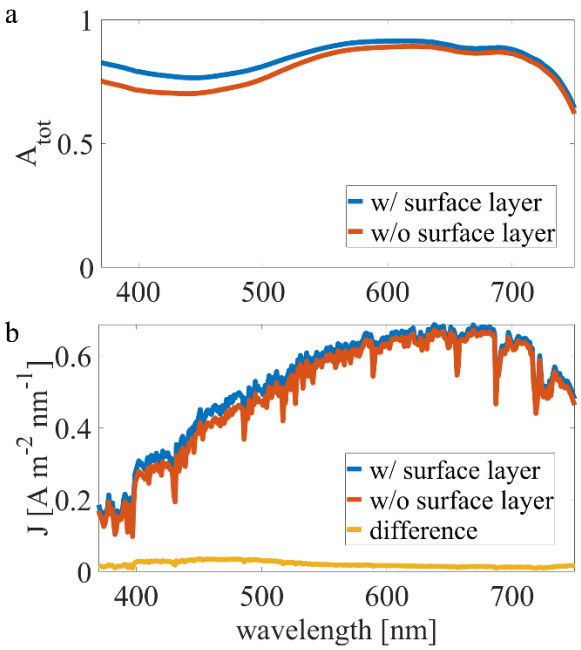


Fig. S13. Rudin-Shapiro sequence on a Fermat's spiral. a) Total absorption in the active layer with and without surface layer. b) Spectral current density with and without surface layer and the difference between the two.

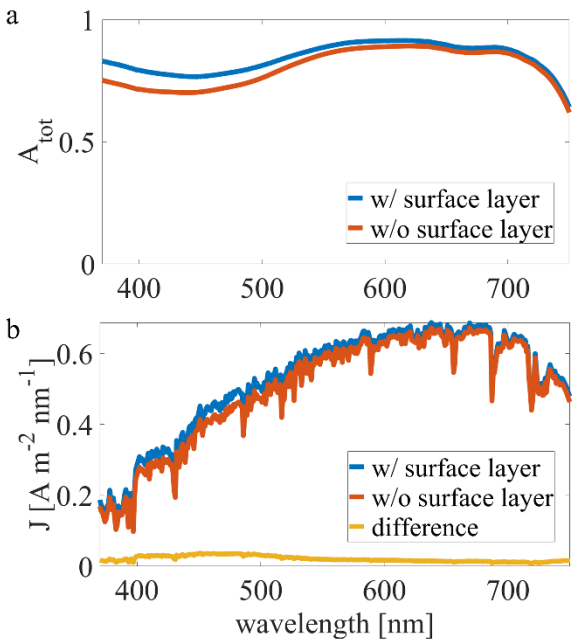


Fig. S14. Thue-Morse sequence on a Fermat's spiral. a) Total absorption in the active layer with and without surface layer. b) Spectral current density with and without surface layer and the difference between the two.

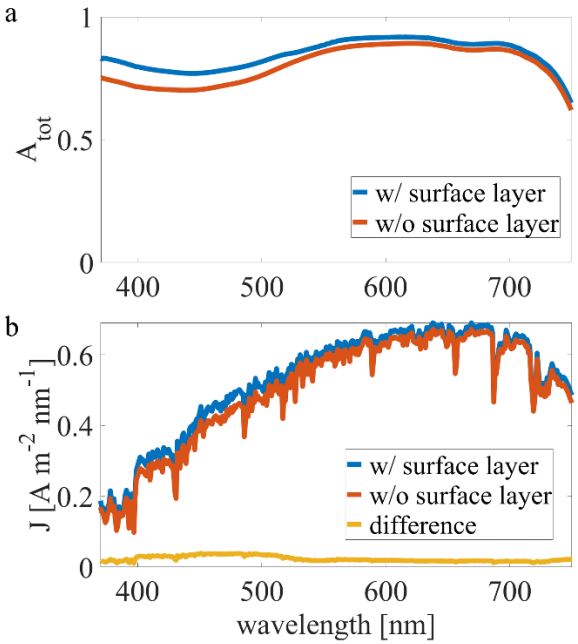


Fig. S15. Periodic sequence on an Archimedean spiral. a) Total absorption in the active layer with and without surface layer. b) Spectral current density with and without surface layer and the difference between the two.

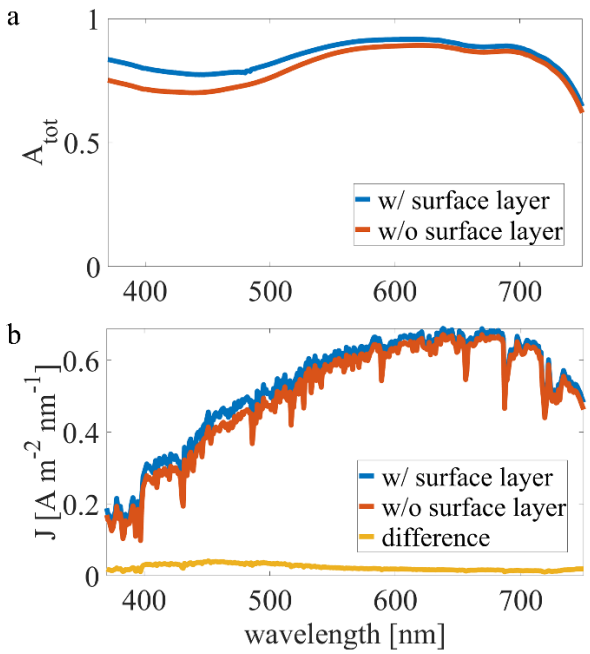


Fig. S16. Rudin-Shapiro sequence on an Archimedean spiral. a) Total absorption in the active layer with and without surface layer. b) Spectral current density with and without surface layer and the difference between the two.